Journal of Radiotherapy in Practice

Journal of Radiotherapy in Practice (2010)
9, 165–174

doi:10.1017/S1460396910000026

Original Article

Aspects of simulator cone-beam CT for radiotherapy treatment planning

Denise Irvine and Mark McJury

Regional Medical Physics Service, Belfast HSC Trust, Belfast, UK

Abstract

Background and purpose: Following a recent major upgrade in cone-beam computed tomography (CBCT) software and functionality, we have reassessed aspects of our Varian Acuity simulator performance for use in treatment planning. The feasibility of using CBCT for treatment planning has been assessed and here we report specifically on Hounsfield number (HN) accuracy and related dose errors, and digitally reconstructed radiograph (DRR) image quality.

Methods: Using a Catphan® 600 CT phantom, HN accuracy and uniformity were investigated for a range of CBCT imaging modes. This included the variation in HNs with scan length and phantom position. Results were compared with those acquired from conventional CT. Treatment plans for three sites were generated using the Rando phantom, and results from CBCT-based data were compared to that from CT-based data using a gamma analysis. Image quality of DRRs based on CBCT data were compared with those from CT data both quantitatively, by calculating the modulation transfer function (MTF) and qualitatively, by counting the number of line pairs visible on a phantom.

Results and conclusions: Catphan data showed that for certain cases, the HN calibration of the Acuity CBCT was out of tolerance and could lead to errors in dose calculation of $>2\%$. HNs were only acceptable for scan lengths >10 cm. In multi-scan mode, geometric shifts and differences in HNs were seen on CT slices on either side of the interface between the two acquisitions. However, comparisons between treatment plans calculated using CBCT data and conventional CT data from Rando phantoms showed that head, pelvis and thorax plans were acceptable. CBCT DRR image quality compared favourably with a conventional CT scanner in some respects; however, image uniformity and low contrast resolution were poorer due to the 'cupping' artefact obtained with CBCT scans.

Keywords

cone-beam CT; simulation; DRRs; CT numbers; Hounsfield numbers; image quality

INTRODUCTION

Modern simulators allow the acquisition of three-dimensional imaging data using cone-beam computed tomography (CBCT) technology. The source and imager rotate around the patient acquiring planar projection views which

Correspondence to: Denise Irvine, Regional Medical Physics Service, Belfast HSC Trust, Lisburn Road, Belfast BT9 7AB, UK. E-mail: denise.irvine@belfasttrust.hscni.net

are reconstructed to form axial scans. Images acquired with the Acuity Simulator (Varian, Palo Alto, CA, USA) in our department, require full rotations around the patient. Scans are acquired in one of two geometries—full-fan scans or half-fan scans. In the case of full-fan scans (for field of view (FOV) <24 cm), the whole of the beam is intercepted by the flat panel imager and is used to reconstruct the axial scans. With half-fan mode (for FOV >24 cm), the flat panel is displaced laterally, with only half the beam used to reconstruct the scans. Different bow-tie filters are used for each scanning geometry and there is a post-patient anti-scatter grid permanently in place.

Typical scan lengths possible (single scanning mode) with 2.5 mm CT slices are 15.5 cm for full-fan geometry and 13.0 cm for half-fan geometry. If longer scan lengths are required, there is an option to image with 'double' or 'triple' CBCT modes. For double scan mode, the inferior region of the scan is acquired first, then the patient's couch is moved longitudinally and the superior region is then acquired. The scans are 'stitched' together during reconstruction. However, due to the diverging cone-beam, there are areas of the patient that will receive higher dose due to the 'overlapping' nature of the acquisitions.

It is well known that CBCT images contain substantial contributions from scattered X-rays.[1–4] This scatter depends on the type of scan, i.e., full-fan or half-fan and the size of the object being imaged. The contribution of scatter to the images will be larger than for a conventional scanner due to the larger cone angle used for CBCT imaging, and if there is a lack of post-patient collimation.[5] This scatter contributes to image noise and can introduce image artefacts and can affect the Hounsfield number (HN) accuracy. Our Acuity simulator has an anti-scatter grid in place above the flat panel imager.

We have recently re-commissioned our simulator following major software upgrade to Acuity ConeBeam CT, version 2.0.11 SP4 (Varian, Palo Alto, CA, USA). A number of aspects of the CBCT imaging system were considered during commissioning, and here we report specifically on the issues which have most impact for treatment planning based on the acquired CBCT data: HN accuracy and digitally reconstructed radiograph (DRR) image quality. In using image data for planning, treatment planning systems (TPSs) perform a conversion of HNs to electron densities. This calibration should be valid for the local CT data, and the TPS may allow some flexibility in conversion. Several planning systems allow manual definition of the calibration, and for the system to have more than one conversion table (Philips Pinnacle, Varian Eclipse, Elekta-CMS Xio). The TPS in use in our department, Oncentra® MasterPlan (Nucletron), has a single algorithm for HN to electron density conversion. It is not designed to be altered by the user and so must be valid for all local CT data. It is therefore important for us, that the HN accuracy was assessed for CBCT scanning, to ensure the HNs were within our range of acceptable tolerances that we apply to our conventional CT scanners in the department. There is considerable literature on CBCT, however, much is concerned with linac-based systems applied to patient setup and online verification. There is comparatively little applied to pre-treatment imaging and the implications for use of the data in treatment planning.

METHODS

HNs

On our Acuity Simulator (Varian), a number of potential imaging modes are available for CBCT, but only two were commissioned at installation: (i) standard dose, 150 cm; (ii) multi-scan mode, 150 cm; where, 150 cm refers to the source to imager distance.

This Varian nomenclature is slightly awkward in that both modes allow single-scan and multi-scan acquisitions. The difference between the modes related to the exposure factors (kV and mAs), leading to differences in dose and image quality. The multi-scan mode has a lower mAs setting to reduce the anode heat levels achieved during the scan. This is particularly useful when using the 'double' or 'triple' scanning modes.

https://doi.org/10.1017/S1460396910000026 Published online by Cambridge University Press

Image data from the CBCT may be used for dose calculation in the TPS. Dose calculation uses electron densities derived from image HNs, so firstly we assessed HN accuracy. This was carried out using a Catphan® 600 CT phantom (the Phantom Laboratory, Inc., Salem, NY, USA). The Catphan phantom was scanned in a conventional Siemens CT scanner (Siemens Emotion 6) using a number of different protocols used clinically and the HNs for each insert measured. A measure of the accuracy of the HN calibration is the tolerance of the HN/electron density variation which may lead to a dose error in excess of 2%.[6] We have adopted the method of Kilby et al.[7] where for a 6 MV linac photon beam irradiating a depth of 20 cm of water, 10 cm of lung, or 7 cm of bone, a 2% error in dose is produced with a change of electron density of ± 0.03 for water, ± 0.05 for lung and ± 0.08 for bone. Our TPS uses the relations detailed in Knöös et al.[8] to determine electron densities based on HNs and this formalism was used to generate electron densities and help defining tolerances.

Due to the scatter conditions of the scanner, we firstly investigated the HN accuracy with decreasing scan length and as a function of position of the HN module of the Catphan CT phantom within the cone-beam.

We acquired scans of the HN module of the Catphan CT phantom for both full-fan and half-fan scans, with scan lengths ranging from the maximum allowed for a single scan (15.0 cm in the case of full-fan scans and 13.5 cm in the case of half-fan scans) down to 0.5 mm. The HN module was then displaced 7 cm in both the superior and inferior directions for full-fan scans of scan length 15.5 cm and the scans repeated.

In addition to accuracy, HN uniformity was also investigated using module CTP486 of the Catphan CT phantom. Profiles were taken across the central slice of the module and % non-uniformity calculated according to equation 1:

$$\%\text{Non-uniformity} = \frac{(\max - \min)}{(\max + \min)} \times 100 \qquad (1)$$

where max and min represent the maximum and minimum HNs, respectively.

Treatment plans

Using Rando® head, thorax and pelvis phantoms (the Phantom Laboratory, Inc., Salem, NY, USA), three standard treatment plans were generated based on CBCT data. The details of the CBCT acquisitions and the planning parameters are shown in Table 1. The Rando head scan was acquired using the 'single' scan mode, and the thorax and pelvis scans were acquired using the 'double' CBCT mode to achieve longer scan lengths. Similar plans were also generated based on conventional CT data. The three pairs of plans were then compared using gamma analysis generated by the Doselab system (M.D. Anderson Cancer Centre, USA)

DRR image quality

If the CBCT capability is to be used for treatment planning purposes, DRRs would be

Table 1. *Planning parameters and details of the CBCT acquisitions for the Rando phantom scans*

		Head	Pelvis	Thorax
CBCT acquisition parameters	Field of view	24.0 cm (full fan, full bow tie)	40.0 cm (half fan, half bow tie)	40.0 cm (half fan, half bow tie)
	Scanning mode	Standard dose, 150 cm	Standard dose 150 cm	Standard dose 150 cm
	Scan length	15.5 cm	27.0 cm (double CBCT)	27.0 cm (double CBCT)
	Slice spacing	2.5 mm	2.5 mm	2.5 mm
	Matrix size	512 × 512	512 × 512	512 × 512
Treatment planning parameters	Beam energy	6 MV	6 MV	6 MV

CBCT, cone-beam computed tomography.

https://doi.org/10.1017/S1460396910000026 Published online by Cambridge University Press

created from the CBCT data. Treatment verification methods generally involve a quantitative comparison of registered DRR and treatment room image (electronic portal image or EPI). Current generation amorphous silicon portal imagers produce high-quality EPIs, which have replaced film as a gold standard. In reviewing the registered verification images, often the DRR quality is the limiting factor in the quality of the verification. The quality of generated DRRs and source data are therefore crucial for routine verification.

In order to determine the DRR image quality, the Catphan CT phantom was aligned centrally using the lasers, orthogonal to the X-ray beam and scanned at standard clinical settings for both full-fan and half-fan scans at two different slice width/slice spacing combinations (5 mm slices/5 mm spacing and 2.5 mm slices/2.5 mm spacing), and images transferred to the Advantage Sim virtual simulator system (GE Medical Systems). DRRs of each module of the Catphan phantom were created using Advantage Sim, with the gantry and table orientated to 90°. The Advantage Sim system has a sophisticated set of tools for DRR reconstruction. In particular, the reconstruction allows the user to control the depth and range of data included in the reconstruction. For our purposes, we were able to restrict the data range to that of a particular insert, when reconstructing the DRR. Module CTP486 was used to assess image uniformity. Module CTP528 containing bar patterns of up to 21 line pairs per cm was used to assess spatial resolution qualitatively, by counting line pairs, and quantitatively to calculate the modulation transfer function (MTF), based on the method of Droege and Morin[9] as described below. Module CTP515 containing several circular low contrast targets was used to calculate low contrast resolution from sub- and supra-slice targets. Images were analysed using ImageJ version 1.40 g (Wayne Rashband, National Institutes of Health, USA).

DRR High contrast spatial resolution

Using the methodology of Droege and Morin[9] relies on measurement of the standard deviation of the pixel values within the image of cyclic bar patterns.

$$\mathrm{MTF} = \frac{\pi}{\sqrt{2}} \cdot \frac{\sqrt{M^2 - N^2}}{|\mathrm{DRR}_1 - \mathrm{DRR}_2|} \qquad (2)$$

where M = standard deviation (SD) of pixels within bar pattern; N = SD of uniform area of DRR = noise; DRR_1 = mean pixel value of solid portion of phantom; DRR_2 = mean pixel of bar material.

CBCT-based DRRs were compared to DRRs reconstructed from conventional CT data.

RESULTS AND DISCUSSION

HN accuracy

The Catphan CT phantom was scanned in the Siemens CT scanner using a number of different protocols and HN results are shown in Table 2. HNs for each insert were obtained and used to define acceptable ranges (Table 2).

Table 2. *HN values and tolerances derived from the results from the Siemens scanner, the Varian recommended specifications and results obtained using a range of imaging protocols in a conventional CT scanner*

Insert	HN	Min	Max	Varian Spec	Conventional CT scanner range
Air	−1,003	−1,034	−936	−1,000	−1,005 to −992
Teflon	935	849	1,011	990*	930 to 939
Delrin	345	254	416	340	341 to 348
Acrylic	121	79	158	120	119 to 124
Polystyrene	−37	−79	0	−35	−36 to −37
LDPE	−94	−128	−49	−100	−92 to −96
PMP	−184	−217	−138	−200	−182 to −185

CT, computed tomography; HN, Hounsfield number; LDPE, low-density polyethylene; Max, maximum; Min, minimum; PMP, polymethylpentene; Spec, specifications.

https://doi.org/10.1017/S1460396910000026 Published online by Cambridge University Press

The Varian recommended HN calibrations for each insert are also shown in Table 2.

From Table 2, it can be seen that our HNs agree with the Varian recommendations, apart from Teflon, where our average HN is 935 and the Varian recommendation is 990. This is still within our acceptable range for Teflon, though approaching the top of the range. Our CBCT was initially calibrated using the Varian specifications. However, when we started investigating the HN accuracy for different CBCT scans, it became apparent that this calibration was too high and our HNs for Teflon for most scans were out of tolerance. Therefore we recalibrated such that the HN for Teflon was calibrated to 935 Hounsfield Units.

HN variation with decreasing scan length

The HNs obtained for full-fan scans for varying scan lengths for the Standard dose 150 cm mode are shown in Table 3.

From Table 3, for air, polystyrene, low-density polyethylene (LDPE) and polymethylpentene (PMP) inserts, the HNs stay within our acceptable range. However, for Teflon, Delrin and Acrylic, the HNs increase with decreasing scan length and are outside our acceptable range for the shorter scan lengths (boldface denotes values outside of tolerance). We based our tolerances on the HN variation that would lead to a dose error in excess of 2%. This increase in HN for some inserts for small scan lengths is due to the fact that the blades associated with the collimator y-jaws are in a different position than during calibration, and the smaller field length results in less body scatter. Currently, we plan on a single CT slice for our breast treatments, so one potential use of CBCT is to acquire a single slice for radiotherapy planning of the breast. The results show that the HNs are unacceptable for single-slice acquisitions; however, the scans are geometrically accurate and so the single-slice mode could be used if a bulk density is assigned to the patient outline.

Multi-scan CBCT

For scan lengths >15.0 cm (full-fan) and 13.5 cm (half-fan), the 'multi-scan' modes are used. These modes involve making either two ('double CBCT') or three ('triple CBCT') rotations around the patient, with the scans being 'stitched' together during reconstruction. The bed is moved automatically between each positional 'station'. Varian recommends[5] that the double and triple scan modes are not used for full-fan scans because differences in HNs have been reported in each part of the scan. Therefore, we investigated the differences in HN in each part of the scan for half-fan modes. Figure 1 shows a reconstructed anterior–posterior image of the Catphan CT phantom using the double CBCT mode (half-fan). There is an obvious 'step' (see arrow) where the two scans are joined together. Further investigation of this acquisition revealed that the HNs were different above and below this 'join' (see Table 4) with HNs in some cases drifting outside our acceptable range. This 'step' appears when the couch is not calibrated to be exactly 0°, but is still within tolerance (our tolerance on couch position is ±0.5). The 'step' is <2.0 mm in this case.

The calibrated HNs are within tolerance for the single CBCT mode, however, when the

Table 3. *Hounsfield number variation with decreasing scan length for a full-fan scan, standard dose 150 cm*

Scan length (cm)	Air	Teflon	Delrin	Acrylic	Polystyrene	LDPE	PMP
0.5	−999	**1,236**	**461**	**173**	−16	−86	−199
1.0	−999	**1,205**	**452**	**169**	−19	−83	−199
5.0	−999	**1,092**	405	142	−27	−87	−192
10.0	−997	**1,010**	366	118	−39	−93	−191
15.0	−991	939	333	100	−55	−103	−194

Values outside of tolerance are shown in boldface.
LDPE, low-density polyethylene; PMP, polymethylpentene.

https://doi.org/10.1017/S1460396910000026 Published online by Cambridge University Press

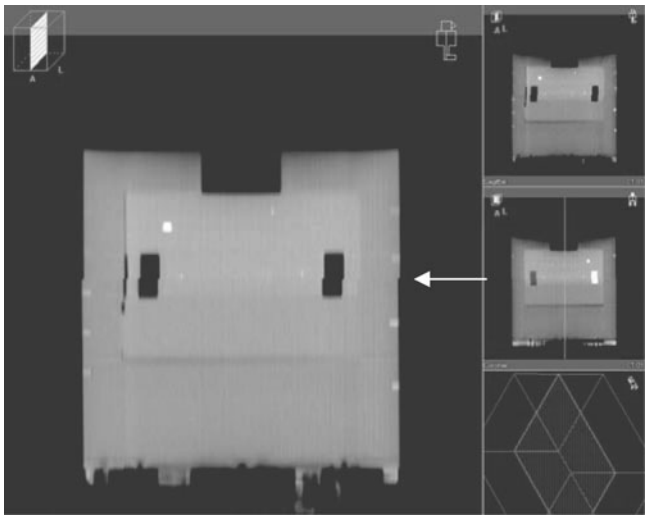

Figure 1. Reconstructed anterior–posterior image of the Catphan CT phantom scanned using the double cone-beam computed tomography mode, with the 'step' artefact arrowed.

Table 4. *HNs measured for 'double' CBCT scans*

	Double CBCT		Single CBCT
	Half-fan (7 cm superior of join)	**Half-fan (7 cm inferior of join)**	**Half-fan (HN module at centre)**
Air	−999	−999	−999
Teflon	**1,054**	954	935
Delrin	383	320	360
Acrylic	138	85	114
Polystyrene	−29	−74	−45
LDPE	−88	**−137**	−102
PMP	−185	**−228**	−193

Values outside of tolerance are shown in boldface.
CBCT, cone-beam computed tomography; HN, Hounsfield number; LDPE, low-density polyethylene; PMP, polymethylpentene.

double CBCT mode is used to obtain an extended coverage, the HNs for Teflon, LDPE and PMP are outside of our acceptable tolerances, and may lead to inaccuracies in dose calculation of >2%.

HN accuracy with varying position within scan length

The HN accuracy was investigated as a function of position within the cone-beam. The HN module of the Catphan CT phantom was displaced 7 cm in both the superior and inferior directions. The total scan length was 15.0 cm. When the position of the module was changed, the HNs remained within ±20 HU of the HNs when the module was placed at the centre of the scan, except in the case of Teflon, which has HNs in the range of dense bone. In this case the maximum difference in HN was −32, but the HN was still within tolerance.

HN uniformity

HN uniformity was investigated for both full-fan and half-fan scans (Figure 2). Non-uniformities are due to both random noise in the image and the 'cupping' artefact due to varying scatter contributions across the field. The 'cupping' artefact is clearly observable on the half-fan

https://doi.org/10.1017/S1460396910000026 Published online by Cambridge University Press

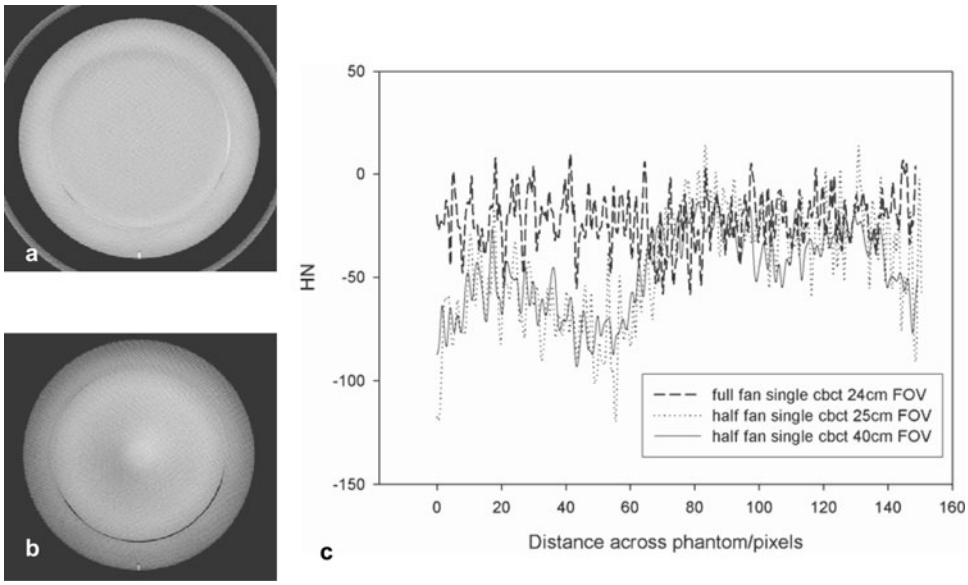

Figure 2. HN uniformity: (a) full-fan scan; (b) half-fan scan; (c) plot of Hounsfield number (HN) against distance across phantom.

scan. Changing the FOV from 25 to 40 cm had no effect on the cupping artefact.

The effect of the 'cupping' artefact can clearly be seen from the plot in Figure 2c. It shows a profile plot of HNs across the uniform Catphan flood-field insert. The dashed line is full-fan CBCT (24 cm FOV), dotted line is half-fan CBCT (25 cm FOV) and solid line is half-fan CBCT (40 cm FOV). This artefact reduces the HNs to levels that could lead to dose errors.

Rando phantom plans

Head/Brain plan

The planning results showed that on all slices at least 98.1% of pixels in the CBCT dose distribution fall within 2 mm/2% of the CT dose distribution. Therefore CBCT data are acceptable for radiotherapy planning of head and neck treatments.

Pelvis plan

Figure 3 shows a comparison of isodose lines obtained on the central slice for the pelvis CT scans (solid lines) and the CBCT scans (dashed lines). An analysis of the standard three-field dose distribution for the pelvis scans found that a minimum of 98.6% of pixels in the (multi-scan) CBCT dose distribution are within 2 mm/2% of the dose distribution obtained for the CT scan. This is also within acceptable tolerance for planning.

Thorax plan

A minimum 98.1% of pixels in the CBCT dose distribution fall within 3%/3 mm of the CT dose distribution. Although the pixel accuracy of the thorax plan results are less accurate than head or pelvis, motional issues will also be a factor for planning in this site. The lower pixel accuracy will be counter-balanced by the improvements in tumour positional accuracy due to the slow acquisition of the CBCT data. A single CBCT acquisition on Acuity takes ~45 s, leading to data which averages out the tumour position, capturing the full motional envelope and enabling more confidence in contouring the full extent of the target and more accurate localisation of the geometric centre. The thorax plans are therefore also acceptable for clinical use.

DRR image quality

Results for spatial resolution, in terms of the number of line pairs visible in each DRR were obtained. Data show that for the CBCT-based DRRs, more lined pairs were visible compared to DRRs produced using CT data.

https://doi.org/10.1017/S1460396910000026 Published online by Cambridge University Press

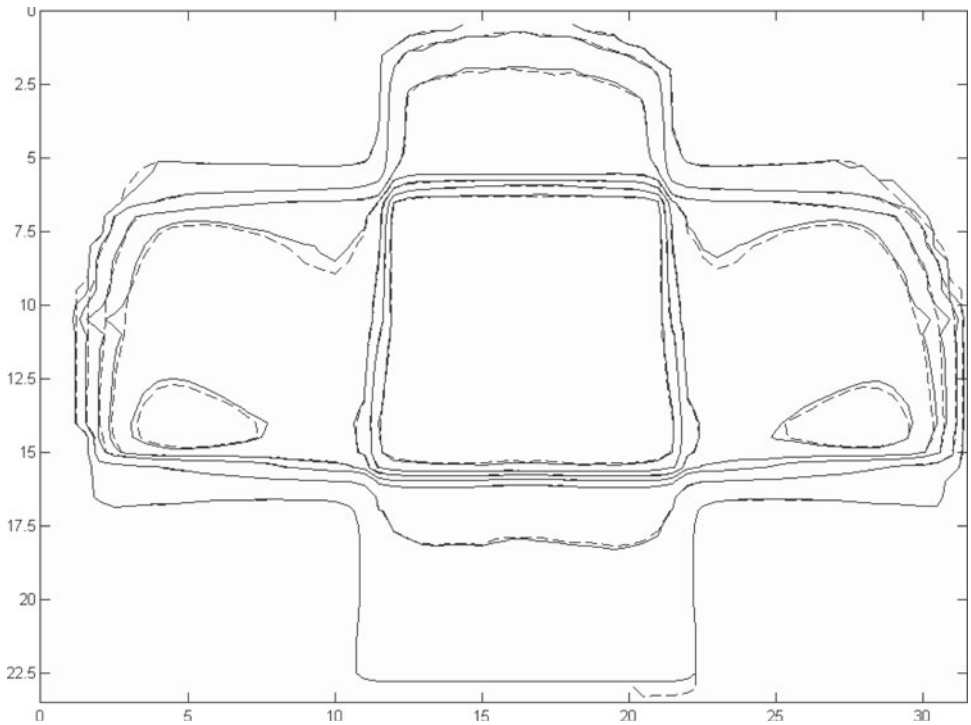

Figure 3. Comparison of isodose lines generated using cone-beam computed tomography and computed tomography data for the Rando phantom pelvis.

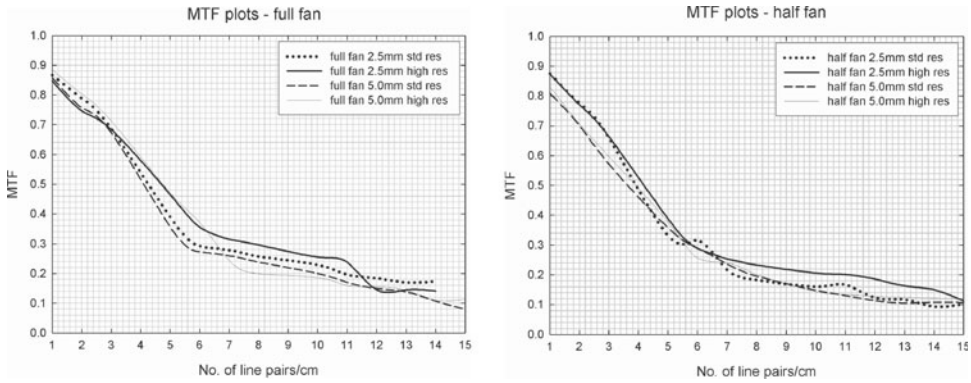

Figure 4. Calculated modulation transfer function (MTF) from bar pattern DRRs. std res, standard resolution; high res, high resolution.

As expected, in the high-resolution DRRs more line pairs were visible. Resolution was also better for full-fan scans compared to half-fan scans. A more objective quantitative assessment was obtained by calculating the MTF (Figure 4). For each DRR, the frequency at which the MTF is 50% of its maximum value was calculated (see Table 5). Also shown in Table 5 are the corresponding results obtained when the same test is carried out in our Siemens Emotion CT scanner.

Image uniformity results are poor for CBCT DRRs (percentage non-uniformities ranged

https://doi.org/10.1017/S1460396910000026 Published online by Cambridge University Press

Table 5. *The frequency for which the modulation transfer function falls to 50% of its value is shown for full and half-fan CBCT imaging modes and for two slice thicknesses (2.5 mm and 5.0 mm)*

Slice width	Full/Half-fan	Resolution	f_{50} (lp/cm) CBCT	f_{50} (lp/cm) Conventional CT
2.5	Full	High	5.3	4.3
2.5	Full	Standard	4.7	3.9
2.5	Half	High	4.6	4.3
2.5	Half	Standard	4.3	3.9
5.0	Full	High	5.2	3.5
5.0	Full	Standard	4.5	3.3
5.0	Half	High	4.6	3.5
5.0	Half	Standard	4.5	3.3

Comparative data are also shown for the conventional Siemens Emotion CT Scanner.
CBCT, cone-beam computed tomography; CT, computed tomography.

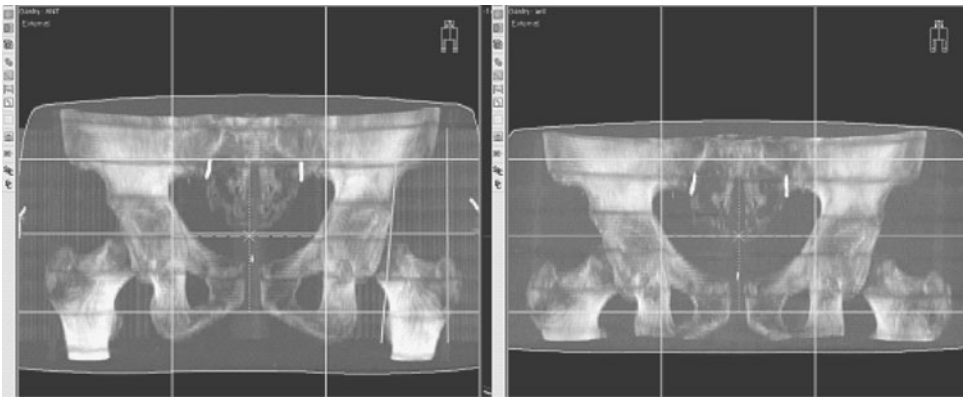

Figure 5. DRRs created from CT data (left) and CBCT data (right). The CBCT DRRs are both geometrically accurate and adequate for the purposes of matching to portal images.

from 15.2 to 25.1%) compared with CT DRRs (percentage non-uniformities were 6% for 2.5 mm slice scans and a maximum of 2% for 5 mm slice scans), due to increased image noise arising from the scatter geometry of the CBCT scanner. Results for low contrast resolution were also poor for CBCT DRRs which was to be expected due to the noise in the images. However, as bone or fiducial markers are generally used for image matching of portal images to DRRs, the DRRs were found to be of acceptable image quality for the purposes of image matching. An assessment of geometric accuracy showed that CBCT DRRs were geometrically accurate to within 2% which is acceptable.

Qualitative DRR tests

DRRs were created for a simple plan using both CT images and CBCT images of the Rando phantom pelvis implanted with gold fiducial markers (Figure 5). A visual inspection of the DRRs shows that the CBCT DRRs compare well with DRRs reconstructed from CT data and that the gold fiducial markers are clearly visible.

CONCLUSIONS

A full assessment of the quality of CBCT data acquired on a Varian Acuity Simulator has been reported. The list of tests carried out is as follows:

https://doi.org/10.1017/S1460396910000026 Published online by Cambridge University Press

1. HN accuracy and uniformity
2. Scan geometry accuracy
3. Performance of multi-scan CBCT modes
4. Comparison with treatment plans calculated using conventional CT scans
5. DRR image quality.

Measurement of HNs showed that HNs were only acceptable for scan lengths >10.0 cm. However, generally scan lengths longer than this are required for treatment planning.

Single-slice acquisitions for breast treatments are one exception. Although our results show that HNs for a single-slice acquisition could lead to unacceptable dose errors, in our department, current practice is to acquire a single CT slice, artificially extend tissue superiorly and inferiorly, and apply bulk density of water to the CT data prior to dose calculation. As the CBCT data are geometrically accurate, the data would be acceptable for our planning protocol.

Varian has recommended[5] that double and triple modes are not used for head scans (full-fan) because differences in HN between the separate scans are unacceptable. An analysis of the treatment plans calculated for the Rando phantom head with a single scan (length 15.5 cm) showed that the resulting dose distribution was acceptable compared with the dose distribution calculated using conventional CT scans.

Half-fan scans (double CBCT) for the pelvis and thorax were found to produce treatment plans that agreed to treatment plans generated from conventional CT data to within 2% at the 2 mm/2%, and 2% at the 3 mm/3% criterion, respectively. All scans were found to be geometrically accurate and the DRRs were of sufficient image quality for image matching. Although HN values drift out of tolerance at scan interfaces in multi-scan CBCT, these differences are not large enough to push the doses of the clinical pelvis and thorax plans out of tolerance.

References

1. Glover GH. Compton scatter effects in CT reconstructions. Med Phys 1982; 9: 860–867.
2. Siewerdsen JH, Jaffray DA. Cone-beam computed tomography with a flat-panel imager: magnitude and effects of x-ray scatter. Med Phys 2001; 28: 220–231.
3. Jarry G, Graham SA, Moseley DJ, Jaffray DJ, Siewerdsen JH, Verhaegen F. Characterization of scattered radiation in kV CBCT images using Monte Carlo simulations. Med Phys 2006; 33: 4320–4329.
4. Ding GX, Duggan DM, Coffey CW. Characteristics of kilovoltage x-ray beams used for cone-beam computed tomography in radiation therapy. Phys Med Biol 2007; 52: 1595–1615.
5. Varian Acuity ConeBeam CT Customer Release Notes, version 2.0, June 2006.
6. Kearns D, McJury M, Commissioning a new CT simulator I: CT simulator hardware. J Radiother Pract 2007; 6: 153–162.
7. Kilby W, Sage J, Rabett V. Tolerance levels for quality assurance of electron density values generated from CT in radiotherapy treatment planning. Phys Med Biol 2002; 47: 1485–1492.
8. Knöös T, Nilsson M, Ahlgren L. A method for conversion of Hounsfield number to electron density and prediction of macroscopic pair production cross-sections. Radiother Oncol 1986; 5: 337–345.
9. Droege RT, Morin RL. A practical method to measure the MTF of CT scanners. Med Phys 1982; 9: 758–760.

https://doi.org/10.1017/S1460396910000026 Published online by Cambridge University Press